ENSO at the Mid-Holocene and LGM: Results from the Paleoclimate Modelling Intercomparison Project PMIP2

Ian Ross, Paul Valdes, Steve Wiggins
University of Bristol, UK

What is ENSO?

El Niño-Southern Oscillation (ENSO) is the strongest mode of interannual variability in Earth's climate. It primarily affects the equatorial Pacific where, every 2-7 years, the mean sea surface temperature (SST) gradient from warm in the west to cool in the east is disrupted, and warm waters flow across the Pacific basin. El Niño affects the climate across the American continent and beyond [1]. The plot ▾ shows monthly equatorial Pacific SSTs for the last 50 years, averaged between 2°S and 2°N [2]. The Pacific mean state has a zonal sea surface and thermocline gradient, conditions maintained by easterly winds along the equator. Imposed on the annual cycle are irregular events, where warmer western Pacific water spills across the whole basin. These events are complicated, depending on subtle interactions between surface conditions and subsurface waves in the equatorial Pacific [3,4].

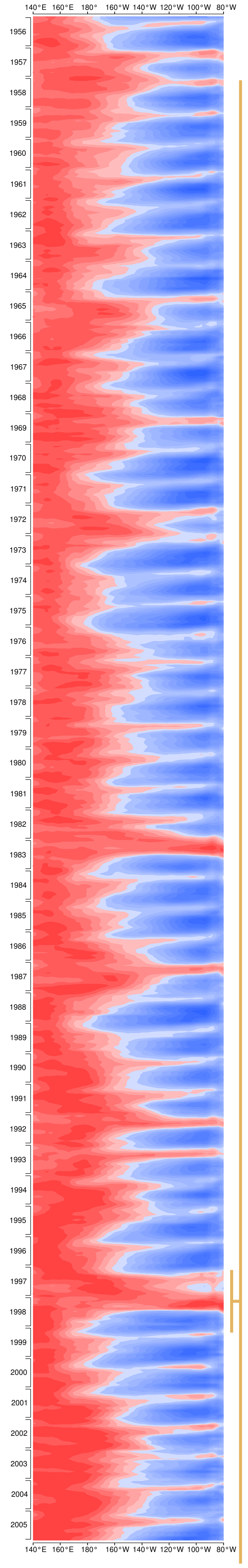

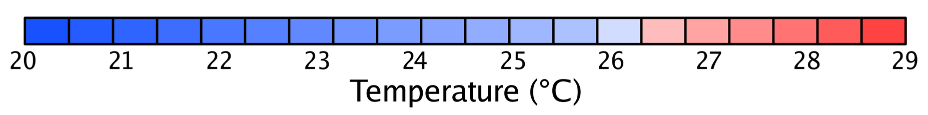

The views below show the evolution through the 1997/98 El Niño of the SST field (horizontal surface – see scale below), surface winds (orange arrows) and equatorial thermocline (yellow curve, projected onto the front of the boxes) [5].

December 1996

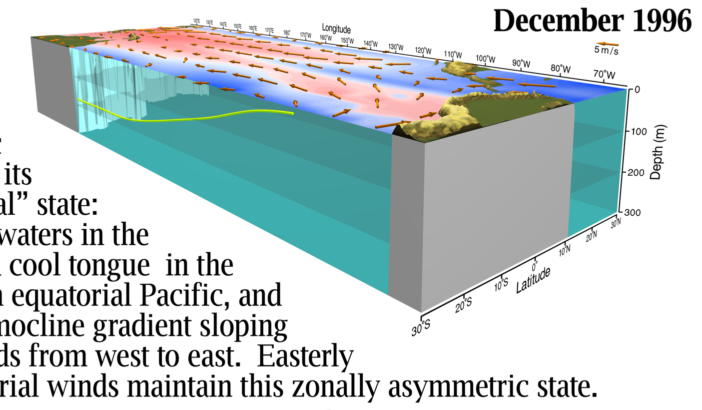

At the end of 1996, the Pacific was in its "neutral" state: warm waters in the west, a cool tongue in the eastern equatorial Pacific, and a thermocline gradient sloping upwards from west to east. Easterly equatorial winds maintain this zonally asymmetric state.

June 1997

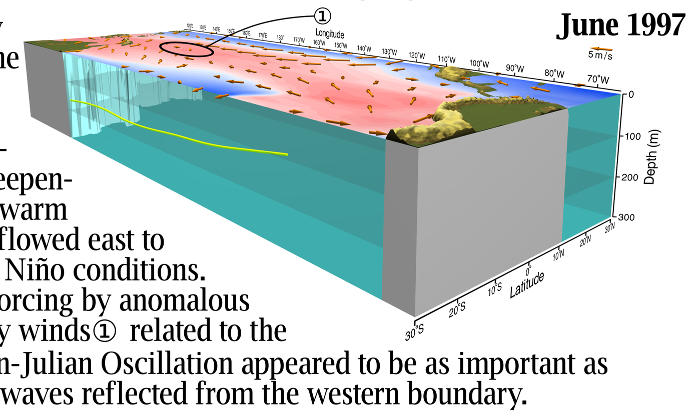

In early 1997, the eastern Pacific thermocline deepened and warm waters flowed east to give El Niño conditions. Local forcing by anomalous westerly winds① related to the Madden-Julian Oscillation appeared to be as important as Kelvin waves reflected from the western boundary.

December 1997

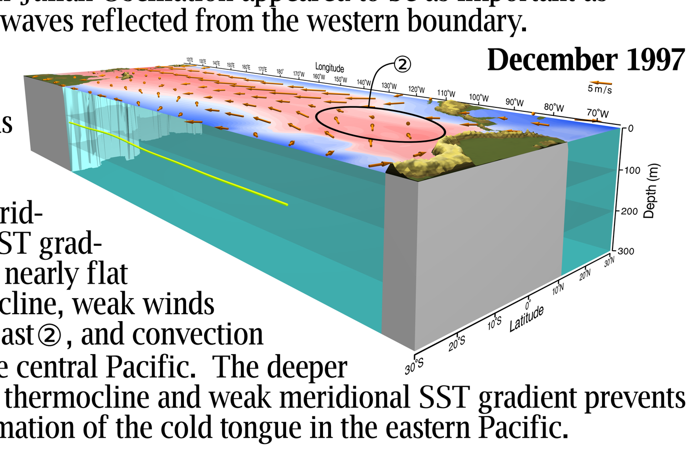

The El Niño state has weak zonal and meridional SST gradients, a nearly flat thermocline, weak winds in the east②, and convection over the central Pacific. The deeper eastern thermocline and weak meridional SST gradient prevents the formation of the cold tongue in the eastern Pacific.

March 1998

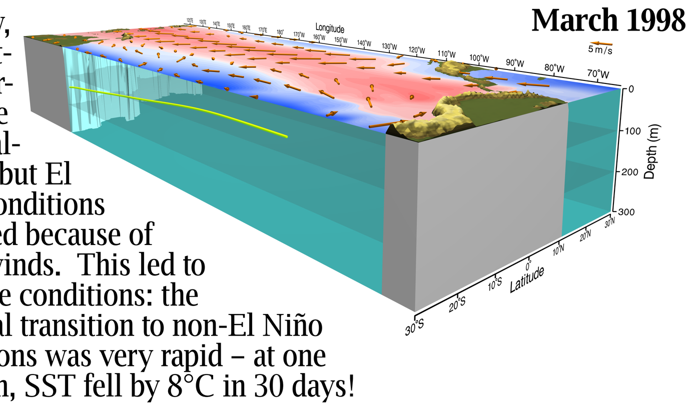

By now, the eastern thermocline had shallowed, but El Niño conditions persisted because of weak winds. This led to unstable conditions: the eventual transition to non-El Niño conditions was very rapid – at one location, SST fell by 8°C in 30 days!

June 1998

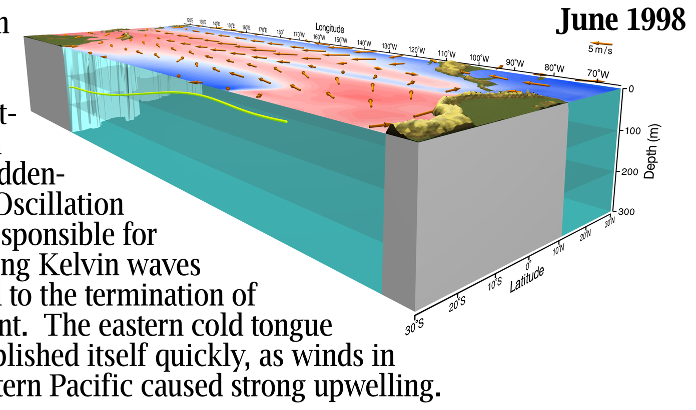

Western Pacific winds associated with the Madden-Julian Oscillation were responsible for triggering Kelvin waves that led to the termination of the event. The eastern cold tongue re-established itself quickly, as winds in the eastern Pacific caused strong upwelling.

December 1998

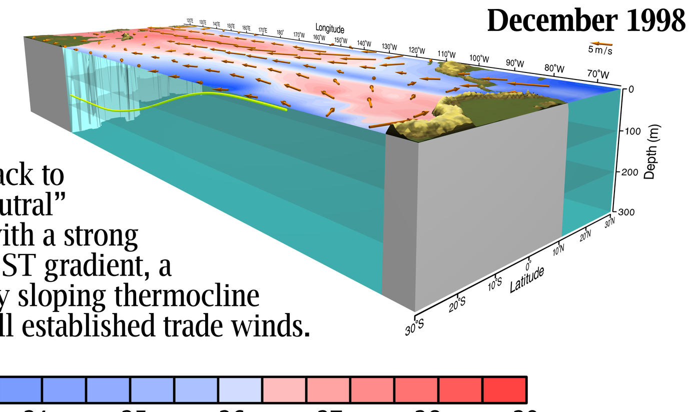

By the end of 1998, conditions were back to the "neutral" state, with a strong zonal SST gradient, a strongly sloping thermocline and well established trade winds.

The PMIP2 Models and Simulations

The second phase of the Paleoclimate Modelling Intercomparison Project (PMIP2) collected results for pre-industrial, mid-Holocene and Last Glacial Maximum conditions from a range of fully coupled atmosphere-ocean general circulation models [6]. The models ▸ use different modelling approaches, and different spatial resolutions and parameterisation schemes in both atmosphere and ocean. They vary widely in the fidelity with which they simulate modern climate and in the extent of modifications made to simulate the paleoclimate conditions.

Results shown here are from simulations with fixed terrestrial vegetation. Based on studies of the mid-Holocene West African monsoon, vegetation feedbacks are likely to have an important but relatively small impact in the Pacific [7]. It will be straightforward to determine the effects on ENSO simulations of dynamic vegetation, and this will be done later.

Modelling group	Model name	AGCM resolution	OGCM resolution	Length of run (years) Modern	6ka	21ka	Line style
National Center for Atmospheric Research (NCAR)	CCSM	T42 L18	320 × 395 L40	50	50	50	
LASG/Institute of Atmospheric Physics, China	FGOALS-1.0g	128 × 60 L26	360 × 170 L33	100	100	100	
University of Wisconsin; University of Bristol, UK	FOAM	R15 L18	128 × 128 L24	100	100		
Goddard Institute for Space Studies (GISS)	GISSmodelE	72 × 46 L15	72 × 46 L13	50	50		
Hadley Centre, UK Meteorological Office; University of Bristol, UK	HadCM3M2 UBRIS-HadCM3M2	2.5° × 3.75° L19	1.25° × 1.25° L20	100 100	 100	100	
Institut Pierre Simon Laplace	IPSL-CM4	2.5° × 3.75° L19	ca. 2° × 2° L20	100	100	100	
Center for Climate System Research (University of Tokyo); National Institute for Environmental Studies; Frontier Research Center for Global Change (JAMSTEC)	MIROC3.2	T42 L20	256 × 192 L44	100	100	100	
Meteorological Research Institute, Japan Meteorological Agency	MRI-CGCM2.3.4fa MRI-CGCM2.3.4nfa	T42 L30	2.5° × 2° L23	100 100	100 100		

All simulations were performed under common forcing conditions. Boundary conditions ▾ for the PMIP2 simulations are fairly standard for this sort of work. The main difference between the modern and mid-Holocene simulations is the orbital parameters – perihelion now occurs in boreal winter, but was closer to boreal summer in the mid-Holocene, so the seasonal cycle of Northern Hemisphere insolation was stronger than today. For the LGM, atmospheric CO_2 concentrations were lower and extensive ice sheets covered much of the Northern Hemisphere [8].

Boundary condition		Modern	6ka	21ka
Ice sheets		Modern	Modern	**ICE-5G**
Topography/coastlines		Modern	Modern	**ICE-5G**
Greenhouse gases:	CO_2	280 ppm	280 ppm	**185 ppm**
	CH_4	760 ppb	650 ppb	**350 ppb**
	N_2O	270 ppb	270 ppb	200 ppb
Insolation:	Solar constant	1365 Wm^{-2}	1365 Wm^{-2}	1365 Wm^{-2}
	Eccentricity	0.0167245	0.018682	0.018994
	Obliquity	23.446°	24.105°	22.949°
	Angular precession	102.04°	**0.87°**	114.42°

Modern Results

Model results are compared with NOAA ERSST and NCEP reanalysis datasets [2,9]. For assessing ENSO variability, the observational record is quite short – perhaps 100 years of reliable SST data, and less atmospheric data. The Pacific climate is a moving target: there is a mid-1970s shift in ENSO behaviour and decadal variability throughout the record. This makes it difficult to decide whether a model adequately simulates "modern ENSO". The 25 El Niños since 1900 differ in intensity and were probably initiated and terminated by different mechanisms: the sample is too small to develop a taxonomy of El Niños or select a "typical" El Niño. To make some progress, we assume that the observations do represent a reasonable target against which to compare our models. The plots ▸▸ show mean climatology and variability of Pacific SST anomalies. Also shown is the power spectrum of NINO3 index variability (SST anomaly, 150°W-90°W, 5°S-5°N, a measure of how El Niño-like conditions are). The table ▾ displays zonal mean Pacific SSTs, ENSO variability measured by the NINO3 index and Walker/NINO3 index correlation. (The Walker index is normalised vertical pressure velocity difference between the west and central Pacific.) Observational indexes are negatively correlated, reflecting the association of regions of high SST with strong convection.

Model	Zonal mean equatorial Pacific SST (°C)	NINO3 standard deviation (°C)	Walker/NINO3 index correlation
Observations	27.16	1.20	-0.73
pre-1976	27.08	1.17	-0.76
post-1976	27.48	1.25	-0.85
CCSM	26.16	1.23	-0.29
FGOALS-1.0g	25.63	1.95	-0.37
FOAM	21.39	1.76	-0.21
GISSmodelE	28.53	0.30	
HadCM3M2	26.76	0.85	0.50
IPSL-CM4	26.98	1.21	-0.02
MIROC3.2	25.93	1.15	
MRI-CGCM2.3.4fa	26.18	0.98	-0.45
MRI-CGCM2.3.4nfa	23.36	1.54	0.28
UBRIS-HadCM3M2	26.30	1.26	0.37

The failure to represent the coupling between ocean temperatures and convective motions of the lower atmosphere is a common feature of coupled ocean-atmosphere GCMs. It is related to a failure to capture the asymmetry of the ITCZ in the Pacific – models ▾ exhibit a double Pacific ITCZ, while the real ITCZ never migrates south of the equator. The cause of this is not fully understood, but is probably due to inadequate modelling of stratus clouds.

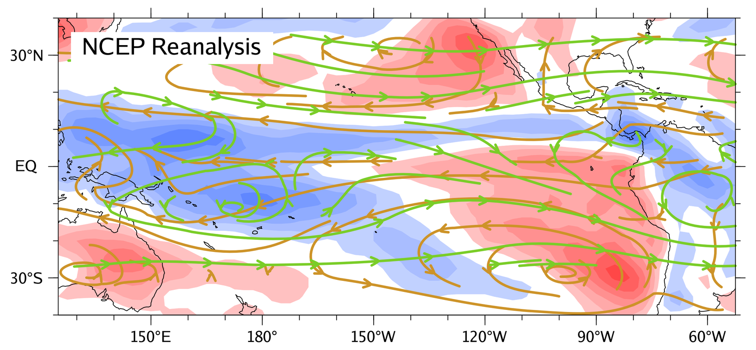

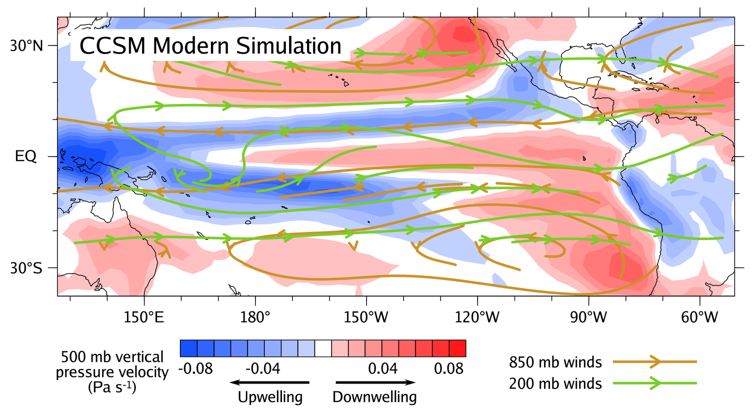

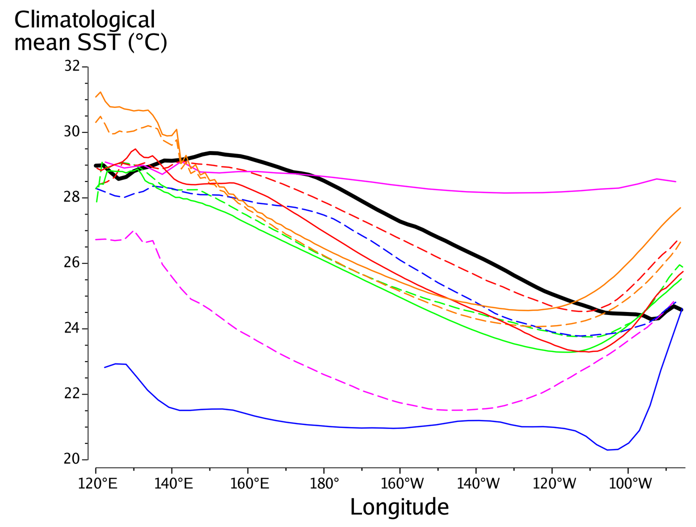

Earlier studies showed that skill in simulating ENSO variability is closely tied to the accuracy of the simulated base Pacific climatology [10]. One essential control on ENSO dynamics is the Pacific zonal SST gradient: here ▴ we show mean SST between 2°S and 2°N across the Pacific. (On all line plots here, black shows observations and coloured lines model results, using the colour code in "The PMIP2 Models and Simulations".) The models generally capture the zonal SST gradient well, except east of about 120°W. Eastern equatorial Pacific surface conditions are controlled by upwelling of cool water from below the shallow eastern thermocline and the effects of marine stratus clouds, neither of which are easy to model. Most models overpredict SSTs in the eastern Pacific, pointing to problems with stratus clouds, which act to cool the sea surface – their presence is essential for the establishment of the eastern equatorial cold tongue during boreal summer.

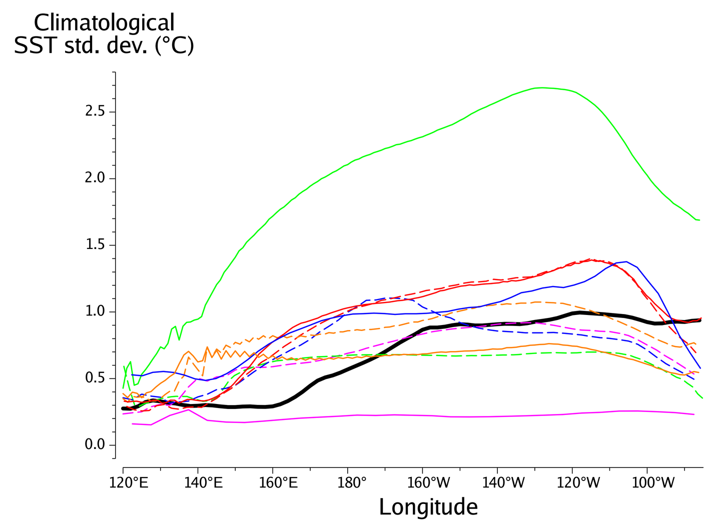

SST variability increases from west to east across the Pacific. Here ▴ we show the standard deviation of SST anomalies averaged between 2°S and 2°N. Strong eastern variability is tied to thermocline fluctuations, while the deep warm pool in the west damps the effects of El Niños. To a large extent, the models capture the variability gradient, although there are problems in the east, with a consistent under-prediction of variability. This is probably a result of stratus cloud problems again – such clouds are a source of variability in the eastern Pacific, and under-prediction of variability tends to be associated with over-prediction of mean SSTs. Examination of the modelled cloud fields would help to sort this out.

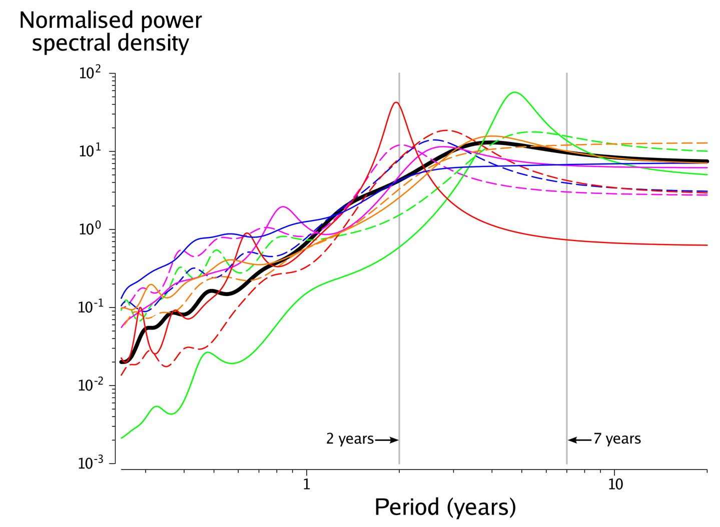

The spectrum of interannual eastern Pacific SST variation ▴ shows a broad peak at periods of 2-7 years; many of the models display similar variability, but few get the frequency quite right. There has been a definite tendency to improvement in this aspect of coupled models: fewer models show strong biannual variability than in past comparisons [11].

Other analyses [in preparation - ask if you're interested] reveal more problems in the representation of ENSO in the models. Examination of El Niño/La Niña asymmetry [12] indicates that, at least to some extent, the representation of this important feature of the Pacific climate is unrelated to the fidelity of the base climatology. This should serve as something of a warning against trying to infer too much from models with clear deficiencies!

Paleoclimate Results

The Mid-Holocene (6 kyr BP)

Reconstruction of ENSO mid-Holocene variability from paleoproxy data is reasonably conclusive that the intensity and frequency of El Niño were both lower than today. This is inferred from coral and lake records with annual layering [17,18,19,20], consistent with an increased zonal SST gradient reconstructed from ocean sediment cores [13,14]. Weaker El Niño also fits northern Australia precipitation records – with less and weaker El Niños, the centre of tropical Pacific convection and rainfall remains in the western Pacific, so conditions there are wetter [15,16].

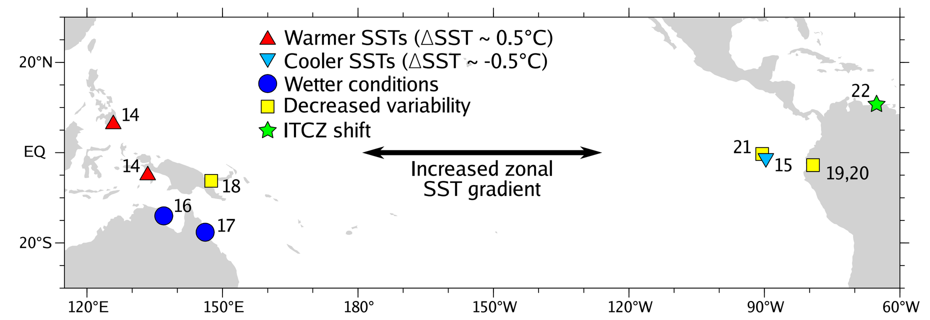

Despite this simple explanation, the existence of annually resolved paleoproxy records is critical for inferring a reduction in ENSO variability. Changes in the mean Pacific climate do not translate directly into changes in ENSO.

The mechanisms for the mid-Holocene weakening of ENSO are relatively straightforward: the boreal summer perihelion led to a stronger seasonal cycle of insolation in the northern hemisphere which strengthened the Asian monsoon system. Monsoonal wind convergence in the western Pacific led to intensified easterly trade winds near the equator, strengthening the zonal thermocline gradient, stabilising "neutral" conditions and suppressing El Niño.

The models are almost unanimous in predicting a decrease in ENSO variability at the mid-Holocene, but the deficiencies noted in the modern simulations persist and details of the modern to mid-Holocene changes vary.

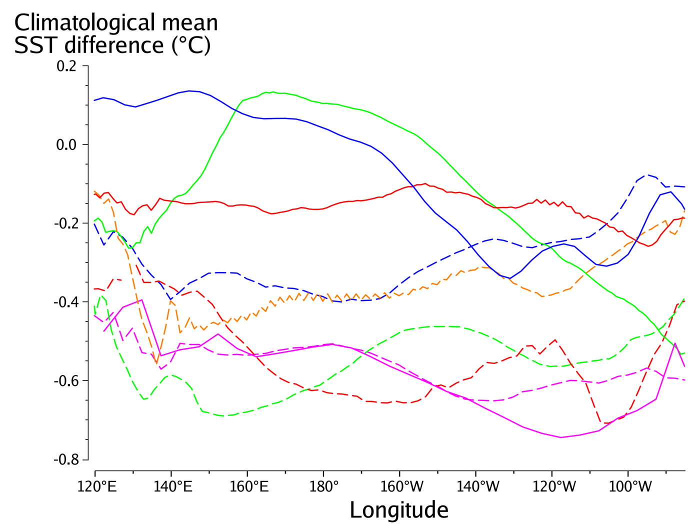

Mid-Holocene/modern ΔSST ▴ across Pacific: some models show an enhanced zonal SST gradient as expected from the paleoproxy data. All of the models show ▴ a reduced mean SST in the equatorial Pacific at the mid-Holocene, and there is an almost unanimous reduction in ENSO variability. This is despite the wide variation in biases in modern mean climatologies across the models. The mid-Holocene NINO3 power spectra show ▴ little change. Some models have a small reduction in ENSO frequency, but the shifts are tiny.

Model	Zonal mean equatorial Pacific SST (°C)	NINO3 standard deviation (°C)
CCSM	26.01 (-0.15)	0.97 (-0.26)
FGOALS-1.0g	25.51 (-0.12)	1.78 (-0.17)
FOAM	21.31 (-0.08)	1.45 (-0.31)
GISSmodelE	27.94 (-0.59)	0.30 (+0.00)
IPSL-CM4	26.41 (-0.57)	1.09 (-0.12)
MIROC3.2	25.38 (-0.55)	0.77 (-0.38)
MRI-CGCM2.3.4fa	25.90 (-0.28)	0.72 (-0.26)
MRI-CGCM2.3.4nfa	22.80 (-0.56)	1.18 (-0.36)
UBRIS-HadCM3M2	25.94 (-0.36)	0.84 (-0.42)

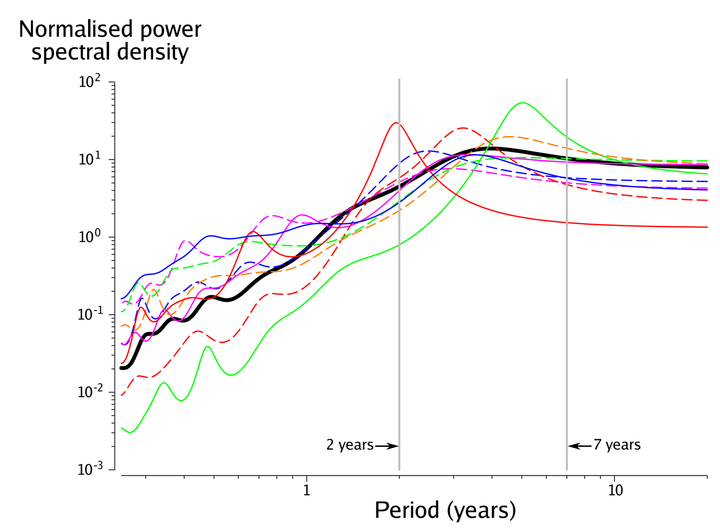

The Last Glacial Maximum (21 kyr BP)

There is no LGM ENSO paleoproxy data: no known exposed LGM corals, and no known varved lake sediments in the equatorial Pacific. This is a disaster for LGM ENSO model/data comparison! The usual tactic is to look at the mean ocean state, derived from low-resolution marine sediments, and to try to infer ENSO variability. There are two problems with this.

First, reconstructions of LGM Pacific SSTs are inconsistent. A map ▾ of LGM-modern SST anomalies illustrates the problem. Shown are reconstructed SST anomalies from foraminiferal Mg/Ca ratios (△), alkenone measurements (□), foraminiferal faunal assemblage calculations (☆), all from [22], and reconstructions from foraminiferal $\delta^{18}O$ (◯) [23]. There is little consistency between the different methods beyond broad basin-wide trends. The faunal assemblage values are particularly bad – the data shown here is for the MARGO ANN method – and several ad hoc bias correction approaches have been proposed to help [24,25]. This situation should be ameliorated over the next few years: there are few Pacific Mg/Ca records, but as existing cores are reanalysed using this relatively new method, we will get a clearer picture of the mean ocean state at the LGM.

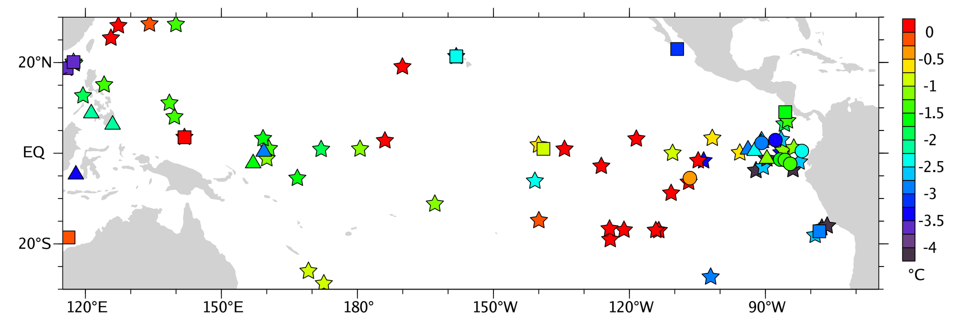

The second problem is that knowing about the mean state of the ocean tells us little about ENSO variability. In the mid-Holocene, we have paleoproxies for both the mean state and variability, allowing us to reconstruct past ENSO behaviour. For the LGM, some studies find a more El Niño-like mean state [23] and "super ENSO" conditions have been proposed [26], but none of this tells us directly about variability in the Pacific.

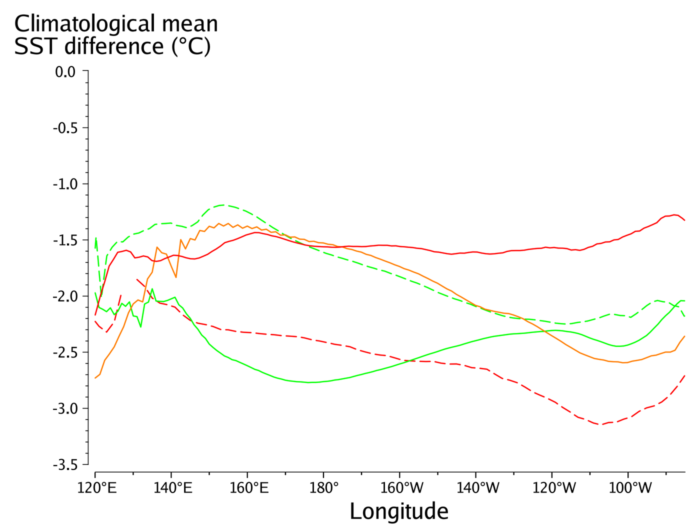

Model	Zonal mean equatorial Pacific SST (°C)	NINO3 standard deviation (°C)
CCSM	24.60 (-1.56)	1.30 (+0.07)
FGOALS-1.0g	23.21 (-2.42)	1.85 (-0.10)
HadCM3M2	24.80 (-1.96)	0.92 (+0.07)
IPSL-CM4	24.40 (-2.58)	1.13 (-0.08)
MIROC3.2	24.14 (-1.79)	1.26 (+0.11)

In the face of this, it is quite hard to interpret the somewhat inconclusive model results ◂ ▴. All models show substantial glacial cooling in the Pacific, but they disagree on the magnitude. Some models show an increased zonal SST gradient at the LGM, some a weaker one (consistent with "super ENSO"), and there is disagreement about whether ENSO variability was stronger or weaker at the LGM than today. Modern-LGM changes in the NINO3 power spectra of the models ▴ are even more inconclusive than for the mid-Holocene.

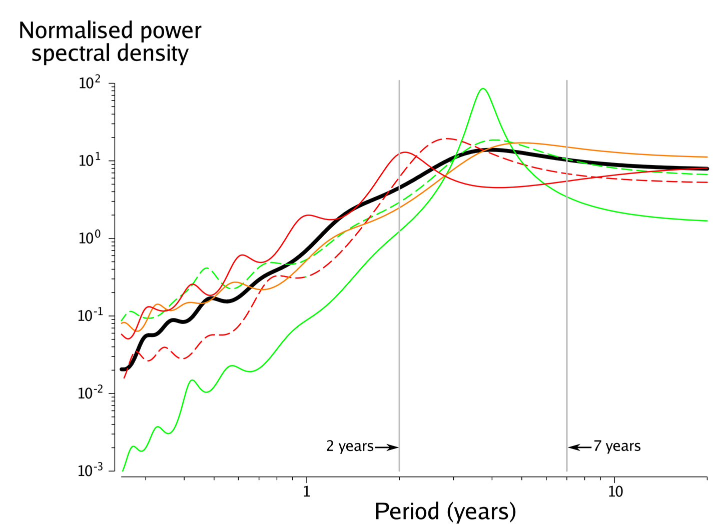

BRIDGE
University of BRISTOL
NATURAL ENVIRONMENT RESEARCH COUNCIL

1 S. G. Philander (1990). El Niño, La Niña and the Southern Oscillation, Academic Press, San Diego.
2 T. M. Smith & R.W. Reynolds (2004). Improved extended reconstruction of SST (1854-1997). *J. Clim.* **17**, 2466-2477.
3 J. D. Neelin et al (1998). ENSO theory. *J. Geophys. Res. Oceans* **103**, 14261-14290.
4 H. A. Dijkstra (2005). Nonlinear Physical Oceanography, 2nd ed., Springer.
5 M. J. McPhaden (1999). Climate oscillations - Genesis and evolution of the 1997-98 El Niño. *Science* **283** (5404), 950-954.
6 PMIP2 web site: `http://www.cea.fr/PMIP2`
7 H. Su & J. D. Neelin (2005). Dynamical mechanisms for African monsoon changes during the mid-Holocene. *J. Geophys. Res. Atmos.* **110**, art. no. D19105.
8 W. R. Peltier (2004). Global glacial isostasy and the surface of the ice-age Earth: the ICE-5G (VM2) model and GRACE. *Ann. Rev. Earth Planet. Sci.* **32**, 111-149.
9 E. Kalnay et al. (1996). The NCEP/NCAR 40-year reanalysis project, *Bull. Amer. Meteor. Soc.* **77**, 437-470.
10 C. R. Mechoso et al. (1995). The seasonal cycle over the tropical Pacific in coupled ocean-atmosphere general circulation models. *Mon. Weather Rev.* **123**, 2825–2838.
11 K. AchutaRao & K. R. Sperber (2006). ENSO simulation in coupled ocean-atmosphere models: are the current models better? *Clim. Dynam.* **27**, 1-15.
12 A. H. Monahan & A. G. Dai (2004). Spatial and temporal structure of ENSO nonlinearity. *J. Clim.* **17**, 3026-3036.
13 L. Stott et al. (2004). Decline of surface temperature and salinity in the western tropical Pacific Ocean in the Holocene epoch. *Nature* **431**, 56-59.
14 A. Koutavas et al. (2002). El Niño-like pattern in ice age tropical Pacific sea surface temperature. *Science* **297**, 226-230.
15 J. Shulmeister & B. G. Lees (1995). Pollen evidence from tropical Australia for the onset of an ENSO-dominated climate at c. 4000 BP. *The Holocene* **5**, 10-18.
16 C. S. M. Turney et al. (2004). Millennial and orbital variations of El Niño/Southern Oscillation and high-latitude climate in the last glacial period. *Nature* **428**, 306-310.
17 A. W. Tudhope et al. (2001). Variability in the El Niño-Southern Oscillation through a glacial-interglacial cycle. *Science* **291**, 1511-1517.
18 D. T. Rodbell et al. (1999). An ~15,000-year record of El Niño-driven alluviation in southwestern Ecuador. *Science* **283**, 516-520.
19 C. M. Moy et al. (2002). Variability of El Niño/Southern Oscillation activity at millennial timescales during the Holocene epoch. *Nature* **420**, 162-165.
20 M. A. Riedinger et al. (2002). A ~6100 14C yr record of El Niño activity from the Galápagos Islands. *J. Paleolimnology* **27**, 1-7.
21 G. H. Haug et al. (2001). Southward migration of the intertropical convergence zone through the Holocene. *Science* **293**, 1304-1308.
22 M. Kucera et al. (2005). Multiproxy approach for the reconstruction of the glacial ocean surface (MARGO). *Quat. Sci. Rev.* **24**, 813-819.
23 A. Koutavas & J. Lynch-Stieglitz (2003). Glacial-interglacial dynamics of the eastern equatorial Pacific cold tongue-Intertropical Convergence Zone system reconstructed from oxygen isotope records. *Paleoceanography* **18**, 1089.
24 A. C. Mix et al. (1999). Foraminiferal faunal estimates of paleotemperature: Circumventing the no-analog problem yields cool ice age tropics. *Paleoceanography* **14**, 350-359.
25 S. Hostetler et al. (2006). Sensitivity of Last Glacial Maximum climate to uncertainties in tropical and subtropical ocean temperatures. *Quat. Sci. Rev.* **25**, 1168-1185.
26 L. Stott et al. (2002). Super ENSO and global climate oscillations at millennial time scales. *Science* **297**, 222-226.